Eur. Phys. J. D **30**, 297–302 (2004)
DOI: 10.1140/epjd/e2004-00099-9

THE EUROPEAN PHYSICAL JOURNAL D

Ground configuration level lifetimes in S-like Ni and Cu ions (Ni XIII and Cu XIV) measured at a heavy-ion storage ring

E. Träbert[1,a], G. Saathoff[2], and A. Wolf[2]

[1] Experimentalphysik III, Fakultät für Physik und Astronomie, Ruhr-Universität Bochum, 44780 Bochum, Germany
[2] Max-Planck-Institut für Kernphysik, 69117 Heidelberg, Germany

Received 30 January 2004 / Received in final form 13 April 2004
Published online 10 August 2004 –

Abstract. Decay curves of the electric-dipole forbidden decay of the $3s^2 3p^4$ ground configuration $^3P_1$ level in the S-like ions of Ni ($Z = 28$) and Cu ($Z = 29$) have been obtained at a heavy-ion storage ring. This completes the earlier measurements on the $^1D_2$ level in Fe ($Z = 26$) and the $^1S_0$ level in Ar ($Z = 18$). The lifetime evaluation process is discussed in the context of structural changes and predicted branching fraction changes along the S I isoelectronic sequence. The experimental lifetime values agree with the results of several calculations.

PACS. 32.70.Cs Oscillator strengths, lifetimes, transition moments – 32.30.Jc Visible and ultraviolet spectra

1 Introduction

In 1942, Edlén [1] identified various prominent lines in the visible spectrum of the solar corona with transitions between levels in the ground configurations of highly charged heavy ions. These transitions are forbidden by the selection rules for electric-dipole (E1) transitions. Only after several more decades they were observed in the laboratory, where they opened an observational window into hot low-density plasmas [2]. Under typical solar coronal conditions, two forbidden lines of iron are prominent, the "red iron line" of Fe X (Cl-like) and the "green iron line" of Fe XIV (Al-like). The transition rates of these two lines have at long last been determined experimentally with an accuracy of 1% or better [3,4]. The iron ions of charge states in between have also been measured, including Fe XI (S-like), but mostly with a somewhat lower accuracy because of more complex level schemes and cascade situations [5,6]. The two 'prominent' iron ions have ionization potentials (I.P.) of about 260 eV and 390 eV [7], respectively. Fe is a particularly abundant element, but not the only one of the iron group showing coronal lines. For example, the S-like ions of Ni and Cu have ionization potentials of 380 eV and 440 eV, respectively, which renders them excitable under coronal conditions, too.

Exactly because of the different situations encountered in different isoelectronic sequences, there are levels that are easier to measure the lifetime of than others. Also, the fine structure intervals vary strongly with the nuclear or the ionic charge, and therefore there are 'windows of opportunity' along an isoelectronic sequence that may be different for the various transitions of interest. In the S I (sulfur) isoelectronic sequence, for example, with its $3s^2 3p^4$ ground configuration, there are 5 levels. The ground state is $^3P_2$. If, in a very rough approximation, the $^3P_{1,0}$ levels lie at an energy x above the ground state, the $^1D_2$ level is near $2x$, and the $^1S_0$ level near $4x$. The interconnecting transitions are not usually covered by one given detection system. We have therefore taken up to observe different ions in the process of obtaining sample data in the S sequence. Ar^{2+} (spectrum Ar III) provided data on the $^1S_0$ level lifetime [8], Fe^{10+} (Fe XI) was available for the lifetime of the $^1D_2$ level [5]. Now Ni^{12+} (Ni XIII) and Cu^{13+} (Cu XIV) have been used to obtain data on the radiative lifetime of the $^3P_1$ level. (The $^3P_0$ level with its predicted lifetime of many seconds (in S-like ions of Ni and Cu) is beyond our present capabilities because of the detector dark rate.) The wavelengths of the transition of interest are in the green and blue for Ni XIII and Cu XIV, respectively, well in the efficiency range of our photomultiplier. The predicted lifetimes are near 6 ms and 4 ms, respectively, which is a convenient range for experiments at a heavy-ion storage ring.

2 Atomic structure background

Atomic structure data are much more complete for ions of elements up to Ni ($Z = 28$) than for heavier ones. Although the ground configuration levels of S-like Cu are

[a] e-mail: traebert@ep3.ruhr-uni-bochum.de

rather well known by now [9,10], this is a fairly recent achievement. Calculations of the transition rates regularly are adjusted to experimental level energies, and most of the calculations to be found in the literature either ended at Ni, or presented data for Cu and beyond without experimental reference data. This may be important, because the sequence of the $3s^2 3p^4\ ^3P_{1,0}$ levels changes between Ni and Cu [9,10], which was not known at the time of the earlier calculations. Saloman and Kim [11,12] have studied in detail how relativistic configurations play a role at various values of the nuclear charge Z; they find that the wave function changes do not necessarily coincide with the level sequence changes. Concerning the various transition rates within the ground configuration, they claim overall good agreement with the preceding work by Mendoza and Zeippen [13] and by Biémont and Hansen [14] (who in turn find good agreement with the early work by McKim-Malville and Berger [15] — 'good agreement' encompasses a factor-of-two agreement for most weak transition rates). Saloman and Kim concentrate on transitions to the ground state, $3s^2 3p^4\ ^3P_2$, and all those transitions appear to follow smooth trends. (The O isoelectronic sequence, with a similar level sequence change between $Z = 23$ and $Z = 24$, and an associated peculiarity of the $2s^2 2p^4\ ^3P_0$ level lifetime, has recently been discussed by Marques et al. [16].) Further calculations have been contributed by Chou et al. [17] and by Bhatia and Doschek [18]. Because of the contradictory literature entries, Ishikawa and Vilkas have performed a new set of calculations for the elements near the ones of present interest [19]. Their accurate approach (with an overall estimate of the $n = 3$ level values of 0.1%) yields level values in close agreement with experiment (with the exception of the $^3P_1$ level in Ga XVI; in this case, their calculation and the isoelectronic trend point to a permutation of digits in the NIST on-line data base (going back to [10]); instead of 38425 cm^{-1} the likely correct table entry would have been 34825 cm^{-1}). (Curiously, the $^3P_0$ level lifetime calculated by Ishikawa and Vilkas [19] is very different from the results obtained by others; this result, in particular for Cu^{13+}, is far away from any isoelectronic regularity and thus in some need of corroboration.)

According to Kaufman and Sugar [7], the decay branch of the $3s^2 3p^4\ ^1D_2$ to the $^3P_1$ level is smaller than 6% of the total for Ni XIII (and the next few lighter ions), but amounts to more than 30% for Cu XIV (and the next few heavier ions). Unfortunately, only few of the available other calculations on the S isoelectronic sequence proceed beyond Ni ($Z = 28$), which arguably is the heaviest element in this sequence that is of astrophysical interest. However, the calculations by Biémont and Hansen [14], the full set of calculations by Saloman and Kim [12], and the calculations by Chou et al. [17] do not show the massive change of the $^1D_2$ level decay branches that the tables by Kaufman and Sugar [7] imply. If that sudden change was real, it ought to show as a notable growing-in cascade in the decay curve of the $^3P_1$ level.

The fact of the level sequence change of the $3s^2 3p^4\ ^3P_{1,0}$ levels is of little importance for the present $^3P_1$ level lifetime study. The predicted lifetime of the $3s^2 3p^4\ ^3P_0$ level is in the range from 5 to 20 s, which is about three orders of magnitude longer than the lifetime of the $^3P_1$ level. In order to detect this slow decay, the cycling pattern of the heavy-ion storage ring would have to be very different from the conditions for best observation of the faster decay. Moreover, the intrinsic noise (dark rate) of the present photodetector renders this device unsuitable for the measurement of such long atomic lifetimes.

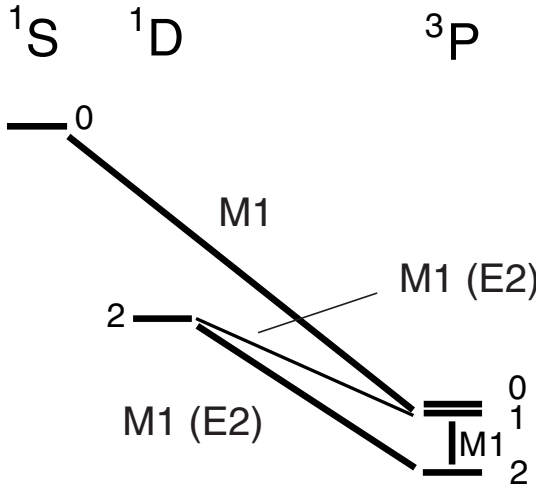

Fig. 1. Schematics of levels and strongest transitions in the $3s^2 3p^4$ ground configuration of S-like ions. For ions of Ni ($Z = 28$) and below, the level sequence of the ground term is $(2, 1, 0)$ (inverted, but regular); for ions from Cu ($Z = 29$) up, the level sequence is $(2, 0, 1)$. All the strong transitions are dominated by magnetic monopole (M1) contributions, whereas electric quadrupole (E2) contributions are much smaller.

In Table 1 we list the various calculational results for the lifetimes of the cascading levels, $^1D_2$ and $^1S_0$ (see also Fig. 1). The decay to the $^3P_1$ level is the dominant decay branch of the $^1S_0$ level; the lifetime is on one hand different enough to be separable in a multi-exponential fit to the $^3P_1$ level decay curve. On the other hand, for Ni XIII and Cu XIV, it is so short as to be close to the short-lifetime limit of the storage ring technique. Consequently this cascade boosts the intensity of the decay of primary interest, but it is difficult to assess from the primary decay curve data. For the $^1D_2$ level, the decay to the $^3P_1$ level is a minor branch. However, the $^1D_2$ and $^3P_1$ level lifetimes are close to each other (less than a factor of two), which severely hampers any multiexponential analyses. Again, if the feeding of the $^3P_1$ level was strong enough, this contribution should show up recognizably in the $^3P_1$ level decay curve, especially with such a marked variation along the isoelectronic sequence as suggested by the Kaufman and Sugar tables [7].

Of course, a direct observation of the $^1D_2$ and $^1S_0$ level decays would be preferable (and neither of them suffers from strong cascade repopulation). However, the major decay branches of the $^1S_0$ level fall into the VUV for which presently no suitable detector is available at any heavy-ion storage ring. The major decay branches of the $^1D_2$

Table 1. Level lifetimes for the $3s^2 3p^4$ levels in the S-like ions Ni XIII and Cu XIV. Experimental findings on the $^3P_1$ level: (a) result of a "naive" single exponential fit (for Cu we show the variation of the result as a function of starting channel); (b) result of multiexponential fits guided by atomic structure information.

Ion	Level	Lifetime (ms) Experiment (this work)	Theory
Ni^{12+}	$^1S_0$		0.432 [15]
			0.391 [13]
			0.387 [7]
			0.393 [14]
			0.3842 [12]
			0.376 [17]
			0.641 [18]
			0.415 [19]
	$^1D_2$		3.89 [15]
			3.61 [13]
			3.618 [7]
			3.60 [14]
			4.286 [12]
			3.723 [17]
			3.60 [18]
			4.000 [19]
	$^3P_0$		18116 [15]
			23952 [13]
			24900 [14]
			22160 [12]
			15870 [17]
			20960 [18]
			133333 [19]
	$^3P_1$	(7.3±0.2) a	6.41 [15]
		(6.50±0.15) b	6.37 [13]
			6.369 [7]
			6.369 [14]
			6.365 [12]
			6.511 [17]
			6.353 [18]
			6.352 [19]
Cu^{13+}	$^1S_0$		0.248 [7]
			0.251 [14]
			0.248 [12]
			0.242 [17]
			0.266 [19]
	$^1D_2$		1.513 [7]
			2.239 [14]
			2.660 [12]
			2.343 [17]
			2.466 [19]
	$^3P_0$		15400 [14]
			15078 [12]
			14490 [17]
			6381621 [19]
	$^3P_1$	(4.15±0.08) - (4.9±0.5) a	3.534 [7]
		(3.60±0.12) b	3.501 [14]
			3.518 [12]
			3.600 [17]
			3.512 [19]

level fall into the UV above the air cut-off and may be reached in a future experiment on S-like ions of Ni and Cu. As mentioned above, the $^1S_0$ level lifetime has been measured in another S-like ion, Ar III [8], employing the very same experimental arrangement at the Heidelberg heavy-ion storage ring. That measurement improved on the data reported from other types of ion traps. The $^1D_2$ level lifetime has also been measured, for S-like Fe [5], and it was found to agree with only some of the predictions. (Among those are the calculations by Biémont and Hansen [14] that also cover the elements of present interest.) The experimental data for Fe XI showed a cascade tail ascribed to $3s^2 3p^3 3d$ levels. While the calculations of those $3d$ level lifetimes for elements up to Fe [20–22] provide some guidance (corroborated by our earlier measurement [5]), none seem to be available for any of the heavier elements.

3 Experiment

Our experiment employed the TSR heavy-ion storage ring at the Max Planck Institute for Nuclear Physics, at Heidelberg, Germany, and used the procedures described previously [5,6]. All ion beams were produced as negative ions from a sputter-type ion source. These ions were then accelerated in the first half of a tandem accelerator, stripped to the desired charge state in a foil stripper, and accelerated further to final energies of about 143 MeV for Ni^{12+}, and 154.5 MeV for Cu^{13+}, respectively. Only a selected-charge state ion beam was transported to and injected into the storage ring. Multiturn injection and stacking of the ions over about 30 turns increased the number of stored ions, so that ion currents in the ring reached up to about 110 μA for Ni^{12+}, and 60 μA for Cu^{13+}. The ions were left coasting for 200 ms. The stored ion beam was then dumped and the procedure repeated.

A few-percent fraction of the ion beam was expected to be in excited levels from the stripping and excitation processes that take place inside the injector. The ion beam travels about 100 m from the injector to the ion storage ring, which at these ion energies takes about 6 μs, that is about twice the revolution time of the ions in the storage ring (circumference 55 m). Injection extended over ≈0.3 ms; the pulsed magnetic field used to inflect the ions settles down at ≈0.8 ms after the start of the injection. The full injection and settling time is faster than the shortest of the expected radiative lifetimes of present interest (which amount to a few milliseconds), but very long compared to all cascade transitions from higher-lying levels above the ground configuration.

After the end of the settling time the ions are stored in stable orbits. The storage time constants (limited by collisional losses) depend on the background gas pressure (here a few times 10^{-11} mbar); they ranged from about 25 to 29 s for the presently studied ions. The actual ion beam current was monitored on-line by a beam profile monitor which detects rest gas ions that are collisionally produced by the circulating ion beam. In principle, the ion beam lifetime is important as a systematic correction of the apparent optical decay data, but in the present case this is

mostly a 3×10^{-4} effect and thus practically negligible. Moreover, relativistic time dilation (with a γ factor near 1.0026 for both of our ions) is almost ten times larger and of opposite sign.

We used optical observation in a side-on geometry, through a sapphire window positioned at a distance of 5 cm from the average ion trajectory. In order to boost the signal rate, a light collection system was employed [24]. This simple trough-shaped reflector (of elliptical cross-section, with the cylinder axis oriented along the beam trajectory) enhances light collection by about a factor of two. The light from Ni (511.6 nm [23]) and Cu (418.3 nm) ions was detected by a 25 mm diameter end-on window photomultiplier tube with an inherent dark rate of less than 30 counts (bi-alkali type EMR 541 N for visible and near-UV light). Interference filters with central wavelengths of 420 nm (bandpass 45 nm), 520 nm (bandpass 50 nm), or 508 nm (bandpass about 5 nm, providing better signal-to-noise than the 520 nm filter, at the cost of a lower transmission), selected a wavelength band near the respective line of interest. Each detection cycle was started about 1 ms before injection, and events were sorted into 1000 bins of 0.1 ms width each.

4 Data evaluation and results

The accumulated data totals are shown in Figure 2; they represent hundreds of independent data sets of one minute accumulation time each that can be recovered from the data records individually. A few of these short-time records corresponded to periods when the injector failed to deliver an ion beam, or technical problems, and these data sets were deleted. For simplicity of evaluation, only the accumulated data sets were analyzed, that are two sets (with different filters) of 180 min and 740 min accumulation time for Ni, and one set of 200 min for Cu. The accumulation time per data channel of 0.1 ms width amounted to about 5.5 s, 22 s, and 6 s, respectively. Although up to 30 000 counts above background were collected in a single decay curve data set (which on its own would permit a lifetime determination to better than 1%), the statistical uncertainty of the fit results was only of the order of 2 to 5%, because of the dark rate of the photomultiplier.

Non-linear least-squares fits of one, two, or three exponential components (plus a constant background) were tried, employing several different algorithms. Fits to various subsets of the data included truncation of the background tail, which yielded no notable differences (that is, no variations larger than expected from straightforward statistical arguments). The data contain data channels that provide an explicit check of the true background: the first channels of each recording show the signal with the old ion sample having been dumped and before the fresh ones are being injected. Therefore the fitting problem was largely reduced to finding a meaningful representation of the curved part of the decay curves above the background level. Neither by eye judgment nor by the χ^2 value did the various fit functions reveal significant differences. The reduced χ^2 values were in the range of 1 to 2.

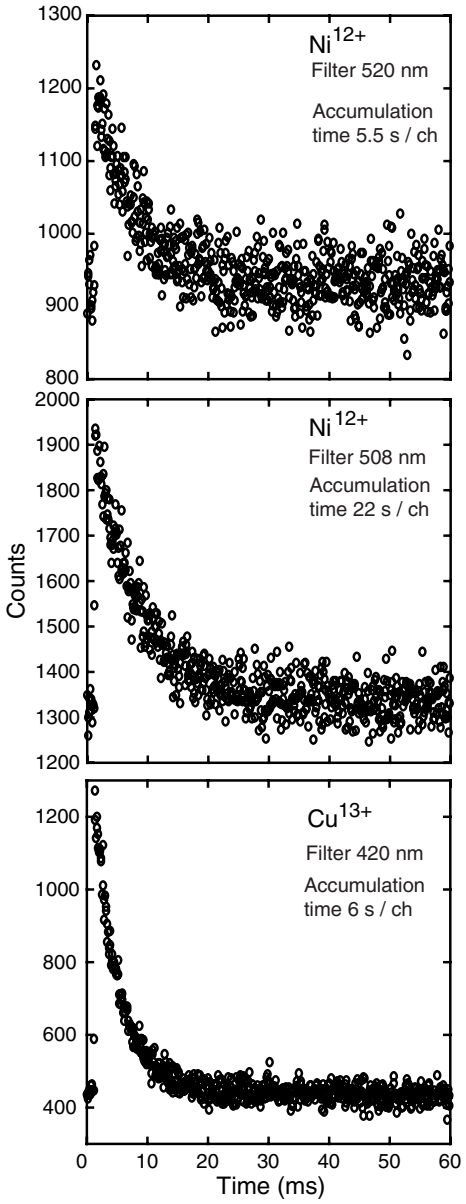

Fig. 2. Decay curves accumulated with Ni^{12+} and Cu^{13+} ions, respectively, coasting in the storage ring. The full data records extend to 100 ms. The interference filter mean wavelength and the accumulation time per data channel (of 0.1 ms width) are indicated individually.

Truncating the very first few channels removes data channels which might be affected by the injection process and the subsequent stabilization of the coasting ion beam in the storage ring. When the evaluation was restricted to data recorded later than 0.5 ms after the end of the injection, the single exponential lifetime results (for increasing starting channel) at first were rather stable and remained within the uncertainty range prescribed by counting statistics. However, the good statistics of the Cu data permitted to extend this truncation of early channels to about 10 ms (almost three primary lifetimes); over this range the result of a single exponential fit increased by

some 10 to 20%. This is a typical sign of the presence of a cascade tail. Anyway, the single-exponential fit lifetime results for both elements were about 20% higher than the majority of the predictions suggested, and already so for early starting channels. Although we show below that this is the result of a considerable systematic error, we include the instructive results from this "naive" single exponential evaluation in Table 1.

Allowing for a second decay component, the fit returned the lifetime of the first component close to the theoretically expected value for the primary decay. The cascade tail was weak, and it was recognizable above the noise only with the two data sets of high statistical reliability. Even then, however, the slow component could not be fitted with a consistent lifetime result. This is reminiscent of the situation encountered with Fe XI [5], where the (much more visible) cascade tail was ascribed to a superposition of several $3d$ level decays.

Moreover, the atomic structure discussed in Section 2 demands the inclusion of decay components that represent the expected cascades from the $^1S_0$ and $^1D_2$ levels. The first of these, with predicted lifetimes of 0.3 ms and less, is comparable in time constant with the injection process. This fast cascade boosts the $^3P_1$ level population, but then quickly dies out. The other cascade is not so different in time constant from the primary decay (less than a factor of two); decay components that close to each other cannot regularly be separated from each other by multiexponential fitting. We tried fits with fixed cascade lifetime typical of the predicted values (like the values given by Biémont and Hansen [14], a calculation that had been corroborated by our $^1D_2$ level lifetime data for Fe XI [5]), and with fixed cascade signal amplitudes (about 5 to 10% of that of the primary decay component). This range is suggested by the calculated branching fractions, the assumption of statistical population of the ground configuration levels, and statistical cascade repopulation from higher-lying levels. Including this growing-in cascade had a major influence on the fit result for the primary decay component, shortening the lifetime by 20 to 30% compared to fits without such a forced growing-in component.

These fit results then fell into the range of predicted lifetime values; the assumptions and educated guesses made in the analysis, however, carry some uncertainty, and consequently the fit result can only be given with a lesser degree of precision. The results for the level lifetimes are given in Table 1. The error estimates exceed the (purely statistical) error bars indicated by the fit routines and reflect the systematic uncertainties discussed above, mainly from using assumed parameters for the growing-in cascade.

5 Discussion

When neglecting cascades, the present lifetime data on ground configuration levels of Ni XIII and Cu XIV (Tab. 1) exceed the available predictions [7,12–15,17,18] for the $3s^2 3p^4\ ^3P_1$ level in the S-like ions Ni XIII and Cu XIV by some 20%. However, simulations of the cascade pattern can be introduced into the decay analysis and then demonstrate that the observed decay curves are compatible with expectation. Although the rates of some (weak) E2 transitions vary among the calculations by up to a factor of two, and some calculated M1 transition rates deviate from the average of other calculations by up to 30%, the predicted level lifetimes of the levels of interest covered by the present measurements differ by much less, and they are largely corroborated by the experimental findings with their uncertainty of about 3%. This accuracy seems quite adequate for most astrophysical applications. Only some atomic physics questions would require higher accuracy and precision.

Most atomic lifetime measurements on heavy-ion storage rings so far have dealt with levels for which cascade contributions were negligible, or were easily separated because of a very different cascade level lifetime. Consequently, remarkably high accuracies (of better than 1%) have been reached that permitted sensitive tests of atomic structure calculations. As has been discussed above, the physical situation (atomic level structure) in the S-like ions is sufficiently complex to prevent a straightforward reliable evaluation of the decay curve of the $3s^2 3p^4\ ^3P_1$ level with a precision that is comparable to the one reached in other cases. Observations of the decay curves of the $^1D_2$ and $^1S_0$ levels in the same ions are called for to establish the cascade lifetimes. A measurement of these cascade level lifetimes would be of merit on its own in testing calculations, and it would help in the analysis of the $^3P_1$ level decay curve when employing a correlated fit, or the ANDC scheme (Arbitrarily Normalized Direct Cascades) [25] that is well established in beam-foil spectroscopy. However, those other decays occur at wavelengths significantly different from the ones of the primary decays of present interest, and some are not yet technically accessible. The same transitions are accessible in lighter ions though, and they have been measured there before [5, 8], so that representative samples for all ground configuration terms in S-like ions have by now been covered by experiment. In this way, calculations can be identified (like those by Biémont and Hansen [14]) that provide numbers in agreement with experiment in all cases tested in the S I isoelectronic sequence.

We are happy to acknowledge the dedicated technical support by the TSR group, in particular by M. Grieser, K. Horn and R. Repnow. ET acknowledges with pleasure the hospitality of the Max Planck Institute for Nuclear Physics, as well as travel support by the Deutsche Forschungsgemeinschaft (DFG). We also acknowledge the loan of optical equipment by A.G. Calamai (Boone, NC, USA) and by P. Beiersdorfer (Livermore, CA, USA).

Note added in proof

Dr. Ishikawa has kindly given additional information on the unexpectedly low decay probability of the $^3P_0$ level in their calculation. Apparently the result communicated to us [19] is from calculations in one of two gauges

(Babushkin/Coulomb); the result of the other is in line with the results obtained by other authors. The discrepancy is subject to further calculational analysis.

References

1. B. Edlén, Z. Astrophysik **22**, 30 (1942)
2. B. Edlén, Phys. Scr. T **8**, 5 (1984)
3. P. Beiersdorfer, E. Träbert, E.H. Pinnington, Astroph. J. **587**, 836 (2003)
4. E. Träbert, Astron. Astrophys. **415**, L39 (2005)
5. E. Träbert, G. Gwinner, A. Wolf, E.J. Knystautas, H.-P. Garnir, X. Tordoir, J. Phys. B: At. Mol. Opt. Phys. **35**, 671 (2002)
6. E. Träbert, A.G. Calamai, G. Gwinner, E.J. Knystautas, E.H. Pinnington, A. Wolf, J. Phys. B: At. Mol. Opt. Phys. **36**, 1129 (2003)
7. V. Kaufman, J. Sugar, J. Phys. Chem. Ref. Data **15**, 321 (1986)
8. E. Träbert, G. Gwinner, Phys. Rev. A **65**, 014501 (2002)
9. J. Sugar, C. Corliss, J. Phys. Chem. Ref. Data **14** (1985), Suppl. 2
10. J. Sugar, V. Kaufman, J. Opt. Soc. Am. B **1**, 218 (1984)
11. E.B. Saloman, Y.-K. Kim, Phys. Rev. A **38**, 577 (1988)
12. E.B. Saloman, Y.-K. Kim, At. Data Nucl. Data Tables **41**, 339 (1989)
13. C. Mendoza, C.J. Zeippen, Mon. Not. R. Astr. Soc. **202**, 981 (1983)
14. E. Biémont, J.E. Hansen, Phys. Scr. **34**, 116 (1986)
15. J. McKim-Malville, R.A. Berger, Planet. Space Sci. **13**, 1131 (1965)
16. J.P. Marques, F. Parente, and P. Indelicato, Hyperfine Interactions **146/147**, 121 (2003)
17. H.S. Chou, J.-Y. Chang, Y.-H. Chang, K.-N. Huang, At. Data Nucl. Data Tables **62**, 77 (1996)
18. A.K. Bhatia, G.A. Doschek, At. Data Nucl. Data Tables **68**, 49 (1998)
19. Y. Ishikawa, M.J. Vilkas, private communication
20. H.E. Mason, H. Nussbaumer, Astron. Astrophys. **546**, 547 (1977)
21. A.K. Bhatia, G.A. Doschek, At. Data Nucl. Data Tables **64**, 183 (1996)
22. S. Fritzsche, C.Z. Dong, E. Träbert, Mon. Not. R. Astron. Soc. **318**, 263 (2000)
23. NIST Atomic Spectra on-line Database at `http://physics.nist.gov/cgi-bin/AtData`
24. J. Doerfert, E. Träbert, A. Wolf, D. Schwalm, O. Uwira, Phys. Rev. Lett. **78**, 4355 (1997)
25. L.J. Curtis, H.G. Berry, J. Bromander, Phys. Lett. A **34**, 169 (1971)